Engineering 6 (2020) 533–540

Contents lists available at ScienceDirect

Engineering

journal homepage: www.elsevier.com/locate/eng

Research
Green Plant Protection Innovation—Article

Rhamnolipids Induced by Glycerol Enhance Dibenzothiophene Biodegradation in *Burkholderia* sp. C3

Camila A. Ortega Ramirez, Abraham Kwan, Qing X. Li *

Department of Molecular Biosciences and Bioengineering, University of Hawaii at Manoa, Honolulu, HI 96822, USA

ARTICLE INFO

Article history:
Received 23 December 2018
Revised 20 May 2019
Accepted 23 July 2019
Available online 25 January 2020

Keywords:
Biodegradation
Bioremediation
Biosurfactant
Biotransformation
Glycerol
Microbial metabolism
Rhamnolipid

ABSTRACT

In highly urbanized areas, pollution from anthropogenic activities has compromised the integrity of the land, decreasing soil availability for agricultural practices. Dibenzothiophene (DBT) is a heterocyclic aromatic hydrocarbon frequently found in urbanized areas, and is often used as a model chemical to study the microbial transformation of pollutants. The potential for human exposure and its health risk makes DBT a chemical of concern; thus, it needs to be environmentally managed. We utilized glycerol to stimulate *Burkholderia* sp. C3 in order to degrade DBT in respect to ① DBT biodegradation kinetics, ② bacterial growth, ③ rhamnolipid (RL) biosynthesis, and ④ RL secretion. Under an optimum glycerol-to-DBT molar ratio, the DBT biodegradation rate constants increased up to 18-fold and enhanced DBT biodegradation by 25%–30% at day 1 relative to cultivation with DBT alone. This enhancement was correlated with an increase in bacterial growth and RL biosynthesis. Proteomics studies revealed the enzymes involved in the upper and main steps of RL biosynthesis. The RL congeners Rha-C10-C10, Rha-Rha-C10-C10, Rha-Rha-C10-C12, and Rha-Rha-C12-C12 were identified in the medium supplemented with glycerol and DBT, whereas only Rha-C12-C12 was identified in cultures without glycerol or with RL inhibitors. The studies indicated that glycerol enhances DBT biodegradation via increased RL synthesis and bacterial growth. The results warrant further studies of environmental biostimulation with glycerol to advance bioremediation technologies and increase soil availability for agricultural purposes.

1. Introduction

Soil and water are essential natural resources for agricultural practices. In highly urbanized areas, pollution from anthropogenic activities has compromised the integrity of agricultural lands and the water streams, leading to decreased soil functionality and food safety concerns. Regions such as North Africa and South Asia have used more than 90% of the available land [1]. In China, the use of polluted water for soil irrigation has resulted in soil pollution [2]. Soil bioremediation can help to restore land for reutilization and crop production. Bioremediation uses microbial metabolisms for the removal of contaminants from the environment [3,4]. Polycyclic aromatic hydrocarbons (PAHs) are a typical class of contaminants from anthropogenic activities [2]. Dibenzothiophene (DBT) is a major sulfur-containing PAH [5] and is often used as a model chemical to assess PAH soil contamination [5]. DBT is a hydrophobic compound with a water solubility of 7.9 $\mu mol \cdot L^{-1}$ and an octanol–water coefficient of 4.44 [6]. The lipophilic nature of DBT allows it to concentrate in the environment and bioaccumulate through the food chain, giving it both a food safety and ecotoxicological risk [7]. Dose-dependent exposure of DBT to zebrafish embryos was found to disrupt cardiac function, with higher doses being associated with morphological abnormalities and mortality [6]. One study showed that DBT and its metabolites act as estrogenic compounds in T47D human breast adenocarcinoma cells [8]. The high detection frequency of DBT in sediments and urbanized areas, the potential for human exposure, and the health threat make it a chemical of concern; thus, DBT needs to be environmentally managed [5,8].

Bioremediation of hydrophobic pollutants such as DBT is frequently limited by the low abundance of microorganisms and by poor chemical bioavailability, resulting in low biodegradation kinetics [9]. In addition to catabolic enzymes [10–12], the intentional augmentation of contaminated soil with microorganisms adept at producing biosurfactants [13,14] is a method to improve

* Corresponding author.
E-mail address: qingl@hawaii.edu (Q.X. Li).

https://doi.org/10.1016/j.eng.2020.01.006

chemical solubilization and bioavailability [15,16]. The production of both biosurfactants and catabolic enzymes in bacteria [17–20] suggests an evolutionary adaptation by microorganisms to overcome low substrate availability.

Burkholderia sp. C3 is a PAH-degrading bacterium isolated from a PAH-polluted site [21]. It contains dioxygenase genes responsible for degrading PAHs such as phenanthrene [22,23]. This study was designed to investigate glycerol as a co-substrate to stimulate the strain C3 to degrade DBT. Our preliminary studies indicated that glycerol can enhance the biodegradation of DBT, unlike other substrates tested (e.g., glucose). Apparent DBT solubilization, foam formation, and earlier DBT degradation by C3 were observed during the cultivation process when glycerol was supplemented. This was not observed in cultures supplemented with DBT alone. Such a difference suggested the secretion of a surfactant agent. Glycerol readily enters into the lipid metabolic pathway of β-oxidation and *de novo* fatty acid synthesis (FAS II), affecting the production of rhamnolipid (RL) biosurfactants and polyhydroxyalkanoic acids (PHAs) [24,25]. There have been few reports on RLs produced by *Burkholderia* sp. To our knowledge, this is the first report on a direct association between RL biosynthesis and DBT biodegradation induced by glycerol. Our studies indicated that biostimulation with glycerol can lead to the effective degradation of DBT in the environment by increasing the bioavailability of hydrophobic contaminants. The technology investigated in the present study may therefore be applicable to the bioremediation of hydrophobic contaminants such as pesticides.

2. Materials and methods

2.1. C3 cultivation and DBT biodegradation

Test tubes were baked at 450 °C for 3 h. DBT dissolved in acetone was placed in a test tube, followed by complete evaporation of acetone under nitrogen (N_2) gas. Next, 5 mL of minimal medium (MM) [26] and an appropriate volume of 50% aqueous glycerol solution were added. The final concentration of DBT was 0.54 mmol·L^{-1} (100 ppm (1 ppm = 10^{-6})), while the final concentration of glycerol was 0, 0.05, 0.5, 5, 50, 200, or 500 mmol·L^{-1}. C3 cells grown overnight in Luria–Bertani (LB) rich medium at 30 °C were washed three times with MM and adjusted to an optical density at 600 nm (OD_{600}) of 0.5 in MM, of which 0.5 mL were inoculated to each of the tubes at a concentration of approximately 0.05 OD_{600}. Cultures with glycerol but without DBT were also prepared. In the RL biosynthesis inhibition experiments, the final concentration of each 2-bromohexanoic acid (HEX) and 2-bromooctanoic acid (OC) was 2 mmol·L^{-1}. Cultures were incubated in a rotary shaker at 30 °C at 200 revolutions per minute. Autoclaved C3 cells were used as controls.

2.2. Extraction and analysis of DBT

DBT was extracted and analyzed according to Ref. [27]. To summarize, after the culture was acidified to approximately pH 2–3 with HCl, DBT was extracted with ethyl acetate three times. The DBT was then analyzed on an Agilent 1100 series high-performance liquid chromatograph (HPLC) equipped with an Aqua C18 column (150 mm × 4.60 mm, 5 μm particle size; Phenomenex, Inc., USA) and detected at 245 nm. The mobile phase was 60% aqueous acetonitrile (ACN).

2.3. Data calculation

Time course points were drawn with standard errors of the mean bars representing variations among three or six biological replicates. Degradation curves were fitted with a first-order kinetic equation, $C = C_0 \times e^{-kt}$, where k is the DBT biodegradation rate constant and C is the concentration measured at time t, and C_0 is the initial concentration (Table 1). The DBT half-life ($t_{1/2}$) was calculated using $t_{1/2} = (\ln 2)/k$. Statistical tests were done with IBM SPSS Statistics 19. The tests performed were Tukey's honestly significant difference (HSD), least significant difference (LSD), and Bonferroni.

2.4. Protein extraction

C3 cells were collected from cultures at day 2 and washed three times with filtered and sterilized distilled water followed by protein extraction, according to the reported method [28] with slight modifications. A lysis buffer was prepared by mixing 9 mL of a 9 mol·L^{-1} urea solution with 1 mL of 10× protease inhibitor solution. Protease inhibitor solution was prepared from Sigma fast protease inhibitor tablets (Sigma-Aldrich, USA). After complete removal of the medium by centrifugation at 5850*g* (g = 9.8 m·s^{-2}), cell pellets were re-suspended in 700 μL of lysis buffer. This cell suspension was added to 300 μL of lysis buffer solution in a screw-cap vial that was 2:3 prefilled with 0.5 mm (diameter) glass beads (BioSpec Products, USA). Cell membranes were disrupted by six cycles of bead-beating at maximum speed for 60 s on a mini-beadbeater (BioSpec Products, USA) and on ice for 60 s. After cell debris removal by centrifugation at 20 820*g* for 15 min, the supernatant was run through an Amicon Ultra-0.5 mL centrifugal filter (3 K cutoff; Millipore, USA) to concentrate proteins on the filter. The filter was then washed with 500 μL of Milli-Q (mQ) water.

2.5. Protein sample preparation for liquid chromatography mass spectrometry analysis

A protein amount of 36 μg was loaded onto a 12% sodium dodecyl sulfate-polyacrylamide gel electrophoresis (SDS-PAGE). The gels were stained with Coomassie blue to visualize the protein bands. Each gel lane was fractionated (approximately 1 mm^3) and washed with 25 mmol·L^{-1} ammonium bicarbonate (NH_4HCO_3)/50% ACN until the pieces became clear. Gel pieces were dehydrated with 100% ACN prior to dithiothreitol reduction at 56 °C for 30 min and iodoacetamide alkylation at ambient temperature for 20 min. In-gel protein digestion was done with Trypsin/Lys-C Mix (Mass-Spec Grade, Promega, USA) at 37 °C for 16–18 h. Protein digests were desalted and concentrated with Pierce C18 tips (Thermo Scientific, USA), and then analyzed on a Bruker nanoLC-amaZon speed ion trap mass spectrometer (MS) system. The peptides were separated on a C18 analytical column (0.1 mm × 150 mm, 3 μm, 200 Å, Bruker, USA) with a gradient elution from 5% to 65% ACN in 0.1% formic acid for 80 min after a 2 min running delay. After 90 min of elution, the mobile phase was changed to 95% ACN containing 0.1% formic acid and remained as such for 10 min, followed by column equilibration with 5% ACN containing 0.1% formic acid for 20 min for the next run. The flow rate was 800 nL·min^{-1}. The MS parameters were set at a capillary voltage of 1600 and a capillary temperature of 149.5 °C. A survey scan from mass-to-charge ratio (m/z) 400 to 3000 was followed by data-dependent tandem mass spectrometry (MS/MS) of the 10 most abundant ions and 0.5 Da instrument error. Dynamic exclusion was set to repeat the same precursor ion twice, followed by excluding it for 0.8 min.

2.6. Protein database and database search

Raw files (file type BAF) were converted to mascot generic format (.mgf) with DataAnalysis software (Bruker, USA). The peak

Table 1
Enhancement of biodegradation rate constant and half-life of DBT is dependent upon glycerol concentrations.

Substrate	Rate constant (d^{-1})	R^2	Half-life (d)	N	Fold change[a]
0.5 mmol·L^{-1} DBT	0.025 ± 0.01	0.63	27.5	30	0
0.05 mmol·L^{-1} glycerol and 0.5 mmol·L^{-1} DBT	0.064 ± 0.01	0.84	10.8	15	1.6
0.5 mmol·L^{-1} glycerol and 0.5 mmol·L^{-1} DBT	0.359 ± 0.09	0.90	1.9	15	13.2[b]
5 mmol·L^{-1} glycerol and 0.5 mmol·L^{-1} DBT	0.390 ± 0.05	0.99	1.8	15	14.5[b]
50 mmol·L^{-1} glycerol and 0.5 mmol·L^{-1} DBT	0.479 ± 0.02	0.99	1.5	30	18.0[b]
200 mmol·L^{-1} glycerol and 0.5 mmol·L^{-1} DBT	0.229 ± 0.02	0.99	3.0	15	8.1[b]
500 mmol·L^{-1} glycerol and 0.5 mmol·L^{-1} DBT	0.113 ± 0.00	1.00	6.1	15	3.5
0.5 mmol·L^{-1} DBT (autoclaved C3 cells)	0.002 ± 0.01	0.31	287.6	27	−0.9
50 mmol·L^{-1} glycerol and 0.5 mmol·L^{-1} DBT (autoclaved C3 cells)	0.009 ± 0.00	0.99	70.44	15	−0.6

Exponential decay equation, $C = C_0 \times e^{-kt}$ was used for fitting "N" data points where k is rate constant and t is time in day; R^2 is the coefficient of determination.
[a] Relative to rate constant of 0.5 mmol·L^{-1} DBT.
[b] Biostimulation at these glycerol concentrations was statistically significant (Tukey HSD; LSD; Bonferroni; $P < 0.001$).

picking algorithm was Apex. The absolute intensity threshold was set to 100.

The canonical and isoform protein sequence (492 entries) database was in FASTA format and was downloaded from the UniProt Knowledgebase (4 April 2016 at 9:35 a.m.). The database was constructed by using *Burkholderia* (UniProt taxonomy: 32008) as the fixed search term and the different protein names as the variable terms. The database search was performed with the MyriMatch search engine [29]. The configuration was as follows: instrument type as ion trap, precursor mass as auto, enzyme as trypsin/P (allowing identification of Trypsin/Lys-C Mix digests), average precursor tolerance 1.5 *m/z*, fragment tolerance at 0.5 *m/z*, and mono precursor tolerance at 10 ppm. The modifications were as follows: carbamidomethyl (fixed) and methionine oxidation (variable).

2.7. Data normalization

Spectral counts of the proteins identified in each treatment were obtained with IdPicker software. The treatments were as follows: (A) 0.54 mmol·L^{-1} DBT; (B) 50 mmol·L^{-1} glycerol; (C) 50 mmol·L^{-1} glycerol and 0.54 mmol·L^{-1} DBT; and (D) 50 mmol·L^{-1} glycerol, 0.54 mmol·L^{-1} DBT, and 2 mmol·L^{-1} OC. The filters to match the peptide to its MS/MS spectra were as follows: a maximum false discovery rate (FDR) of 1% and a minimum of one spectrum per peptide and per match. In order to match peptides to proteins, a minimum of two distinct peptides and spectra and two minimum additional peptides were allowed [30,31]. Data were normalized according to the assumption in Ref. [32]—namely, that MS/MS intensities are equal to 1 and without considering the peptide length. A $\log_{(\text{normalized count} + 1)}$ was applied and the normalized data was compared with the raw data. An analysis of variance (ANOVA, p-value < 0.05) was done to search for protein abundance changes with statistical significance using DEseq [33]. The p-value and log Fold change (FC) of the glycerol × DBT interaction term were calculated and are shown for each protein in Table 2. The log FC represents the effect size of the glycerol × DBT interaction term. When the log FC was upregulated, it indicated that the glycerol × DBT interaction had a positive effect on the protein abundance of the treatments that contained this interaction (i.e., treatments (C) and (D)).

2.8. RL extraction and quantification

RLs were extracted according to Ref. [34]. To summarize, cells were removed at day 2 by centrifugation at 5850*g* for 10 min and filtration with a 0.2 μm pore size. The medium was extracted with ethyl acetate three times. The extracts were combined and dried under a gentle stream of N_2 gas, followed by re-suspending the residues in 0.5 mL of methanol. The same procedure was applied to an RL standard (50 μg·mL^{-1}) dissolved with 5 or 50 mmol·L^{-1} glycerol in MM. RLs were quantified with an orcinol assay [35] (0.19% orcinol (w/v) in 53% sulfuric acid (v/v). A 250 μL aliquot of the sample was collected, dried, and re-suspended in 250 μL of water. To 100 μL of RL extract, or to varying concentrations of a RL standard, a 900 μL aliquot of the orcinol solution was added. Mixtures were incubated for 30 min at 80 °C. Absorbance was read at 421 nm. An RL standard curve was prepared in a range from 0 to 500 μg·mL^{-1}. The remaining 250 μL re-suspended in methanol was used for HPLC fractionation on an Agilent 1100 series HPLC (Agilent Technologies, USA) equipped with an Aqua C18 column (150 mm × 4.60 mm, 5 μm particle size; Phenomenex, Inc., USA) according to Ref. [34]. Two RL fractions were collected at 4–5 min (F1) and 5–6 min (F2) and dried to completion at 45 °C. Fractions were re-suspended in 10 μL of 10% ACN/water and desalted with Pierce C18 tips (Thermo Scientific, USA). The manufacturer protocol was modified as follows: Trifluoroacetic acid was not used. F1 and F2 samples were bound to the C18 tip ten times, washed five times with 5% ACN, and eluted with 10 μL of 70% ACN. Samples were fully dried at 45 °C and re-suspended in 2 μL of 50% ACN containing 40 mg·mL^{-1} of 2,5-dihydroxybenzoic acid (DHB) matrix. A total of 1 μL of matrix was spotted on the target plate and air dried, and then 1 μL of sample/matrix mixture was spotted.

2.9. RL identification

RL congeners were identified on a matrix-assisted laser desorption ionization time-of-flight (MALDI/TOF) ultraflex^{III} mass spectrometer (Bruker, USA) operated in positive, reflectron mode following the published procedures [36]. The instrument was calibrated with the degree of polymerization (DP) series: maltotriose hydrate (DP3, MW: 504.44 g·mol^{-1}), maltotetraose (DP4, MW: 666.57 g·mol^{-1}), maltopentaose (DP5, MW: 828.71 g·mol^{-1}), and maltohexaose (DP6, MW: 990.85 g·mol^{-1}) [37]. A 500 μmol·L^{-1} aliquot of each DP series was dissolved in mQ water. A total of 5 μL of each DP series was mixed with 20 μL of DHB matrix to a final concentration of 62.5 μmol·L^{-1}. A 2 μL aliquot of this mixture was spotted on a MALDI target plate and allowed to air dry. The instrument *m/z* range was 300–1200 with 50 pulsations per laser shot and 38%–50% laser intensity. Ions were suppressed below 300 Da. Flexi Analysis and Compass Isotope Pattern software (Bruker, USA) were used for mass spectral analysis. RL peaks were assigned using an *in silico* database created according to the RLs reported [38], with a 0.5 Da error mass.

An Agilent 6520A liquid chromatograph-quadrupole time-of-flight mass spectrometer (LC-Q-TOF-MS) system (Agilent Technologies, Canada) was used for the MS/MS analysis of samples. The RL sample (20 μL) was separated on a Luna C18 column (100 mm × 2.0 mm, 3 μm particle size) (Phenomenex, Inc., USA) in gradient starting at 5% ACN in 5 mmol·L^{-1} aqueous ammonium formate buffer (pH 3.3) to 95% ACN in 15 min, and then held for

Table 2
Proteins identified mediating RL biosynthesis in *Burkholderia* sp. C3 at day 2 of incubation.

UniProt ID	Protein description	Relative abundance by treatment				log FC	*p*-value
		A	B	C	D		
U1XYV8	HAA synthase (RhlA)	0.85	—	0.86	1.09	1.52	0.090
A0A0B6RU44	Rhamnosyltransferase 1 (RhlB)	1.46	1.02	—	1.28	−0.57	0.407
C4I4U9	RhlB	0.85	0.81	—	1.34	−1.20	0.274
Q3JLM3*	Rhamnosyltransferase 2 (RhlC)	1.00	0.43	—	—	−4.34	0.001[a]
A2RWE5	RhlC	0.94	0.43	—	—	−4.34	0.001[a]
E1TAD4	Phosphoglucomutase/phosphomannomutase (AlgC)	0.45	0.62	0.97	0.54	0.68	0.360
B4ECS6	dTDP-glucose 4,6-dehydratase (RmlB)	—	0.13	0.24	0.27	0.84	0.503
H6TI92	dTDP-4-dehydrorhamnose-3,5-epimerase (RmlC)	1.13	—	0.58	1.24	0.91	0.233
Q2SYI1	dTDP-4-dehydrorhamnose reductase (RmlD)	1.22	0.60	1.10	1.52	2.73	0.030[a]
Q63S87	β-oxoacyl-ACP synthase 2 (FabF)	—	0.62	1.38	—	0.78	0.235
A0A0D5VAR9	3-oxoacyl-ACP-reductase (FabG)	1.32	1.06	1.36	1.45	−0.58	0.328
A0A0D5VAC6	3-hydroxy-ACP-dehydratase (FabZ)	0.98	—	—	1.10	1.39	0.140
K8R0G3	Acyl-CoA dehydrogenase (FadE)	—	—	0.69	—	1.99	0.089
Q3JVY2	Enoyl-CoA hydratase/3-hydroxyacyl-CoA dehydrogenase (FadB)	—	1.15	1.14	—	−0.20	0.768

Treatments were A: 0.5 mmol·L^{-1} DBT; B: 50 mmol·L^{-1} glycerol; C: 50 mmol·L^{-1} glycerol and 0.5 mmol·L^{-1} DBT; D: 50 mmol·L^{-1} glycerol, 0.5 mmol·L^{-1} DBT, and 2 mmol·L^{-1} OC. Three biological replicates were analyzed in each treatment. The mean normalized value was shown in each treatment. The log FC represented the glycerol × DBT interaction term. ACP: acyl carrier protein; CoA: coenzyme A; HAA: 3-hydroxy alkanoic acid.
[a] The changes in relative abundance among treatments showed significant differences ($p < 0.05$).

15 min. The mobile phase flow rate was 0.3 mL·min^{-1}. The column was equilibrated for 10 min between runs. The electrospray ionization interface was set at the negative mode. The capillary voltage was 4000 V. The fragmentor and skimmer voltages were 180 and 80 V, respectively. When the system was in the MS/MS mode, the drying and nebulizing gas was nitrogen, while helium was the collision gas. The gas temperature was 350 °C. The dry gas flow rate was 10 L·min^{-1}. The nebulizer pressure was 25 psi (1 psi = 6.895 kPa). Full-scan data were acquired via scanning from *m/z* 50–1700. The collision energy in the MS/MS mode was 20 eV.

3. Results and discussion

3.1. Biostimulation with glycerol enhances DBT biodegradation and Burkholderia sp. C3 growth

This study was designed to follow a biostimulation strategy to investigate the influence of glycerol on the DBT biodegradation ability of *Burkholderia* sp. C3. Co-substrate experiments with DBT and glycerol exhibited neither a carbon catabolite repression phenomenon nor an antagonistic effect, which has been reported for other co-substrate mixtures [16,39,40]. The results indicate that biostimulation with glycerol supports C3 cell growth while enhancing DBT biodegradation, as shown in Fig. 1. The experiments show that the enhancement of DBT biodegradation was dependent upon the molar ratios of glycerol to DBT used and on the incubation time. Significant differences were observed when the culture was stimulated with 0.5, 5, 50, and 200 mmol·L^{-1} of glycerol (Tukey HSD; LSD; Bonferroni; $p < 0.001$). At these concentrations, glycerol enhanced the DBT biodegradation by 25%–30% after one day of incubation. In cultures at a glycerol (50 mmol·L^{-1})-to-DBT molar ratio of 92.6:1, the strain C3 degraded 100% of 0.54 mmol·L^{-1} (100 ppm) DBT after seven days of incubation. This optimal glycerol concentration was used for the proteomics and mass spectrometry experiments. At this concentration, the DBT half-life decreased to the lowest—from 27.5 to 1.5 days—and the DBT degradation rate constant showed an 18-fold increase (Table 1). Negligible degradation was observed in the control cultures with autoclaved bacteria, as shown by the negative fold change in Table 1. Similar to the DBT biodegradation kinetics at 50 mmol·L^{-1} glycerol supplementation, C3 degraded 92% of 0.54 mmol·L^{-1} DBT at day 10 in cultures containing 0.5 mmol·L^{-1} glycerol. However, at this glycerol concentration, the C3 growth remained at 0.05 OD_{600}, which indicated that the increase in biomass was not the only cause for the enhanced DBT biodegradation, and that additional molecular mechanisms were involved. Statistical analysis showed no significant difference in DBT biodegradation between days 7 and 10 (Tukey HSD; LSD; Bonferroni; $p < 0.05$). Therefore, seven days would be recommended for biodegradation under the conditions tested.

DBT as a sole carbon source did not support strain C3 cell growth. The OD_{600} remained at 0.05 after a 10-day incubation period, which was equal to the initial inoculum (Fig. 1). PAH biodegradation in liquid cultures with a single carbon source depends on the bacterial strain, PAH structures, and PAH concentrations. For example, the strain C3 at day 7 degraded 94% of 40 ppm DBT [22]. Our results indicate that C3 degraded 11%–12% of 100 ppm DBT at day 7. At this concentration, DBT had no apparent benefit to the bacteria, and even a decrease in biodegradation efficiency was observed. This finding was supported by the fact that C3 cell growth in glycerol-DBT mixtures was inhibited in comparison with growth in glycerol alone. For example, mixtures of 0.54 mmol·L^{-1} DBT with glycerol ranging from 50 to 500 mmol·L^{-1} exhibited reduced growth, up to 0.3 OD_{600} relative to glycerol alone, and started after one day of cultivation. DBT did not inhibit growth at lower concentrations of glycerol (0.05–5 mmol·L^{-1}). Growth inhibition with 50 to 500 mmol·L^{-1} of glycerol may be associated with the toxicity of DBT, DBT metabolites, or both. It was reported that PAHs' hydrophobicity and carcinogenicity influence their toxicity [16,41,42].

3.2. The RL biosynthetic pathway is activated in Burkholderia sp. C3

Glycerol is a good carbon source for RL production in *Pseudomonas* species [38]. It can be metabolically assimilated into the lipid pathways affecting PHA granule formation and RL production [24,38,43,44]. Table 2 lists the relative abundance of the enzymes detected in four treatments—namely (A) 0.54 mmol·L^{-1} DBT; (B) 50 mmol·L^{-1} glycerol; (C) 50 mmol·L^{-1} glycerol and 0.54 mmol·L^{-1} DBT; and (D) 50 mmol·L^{-1} glycerol, 0.54 mmol·L^{-1} DBT, and 2 mmol·L^{-1} OC—along with the log FC and *p*-value. These enzymes are responsible for RL biosynthesis, as shown in Fig. 2. Biosynthesis of RLs requires an *R*-3-hydroxydecanoyl-ACP or -CoA lipid precursor produced from the FAS II [45,46] and/or β-oxidation [24] pathways, respectively, and a dTDP-*L*-rhamnose sugar precursor [43]. Once the lipid and sugar precursors are produced, RhlABC mediates the formation of mono- or di-RLs. The anabolic enzymes AlgC and RmlBCD involved in dTDP-*L*-rhamnose biosynthesis were detected

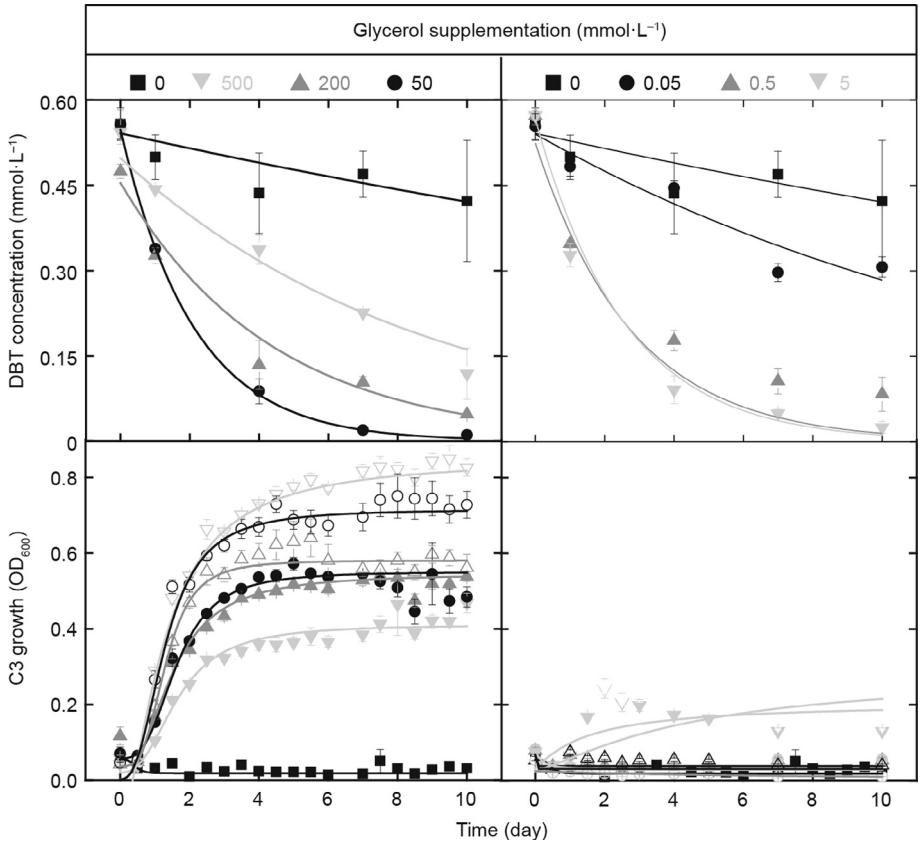

Fig. 1. DBT biodegradation kinetics by *Burkholderia* sp. C3 and its growth over a 10-day cultivation period with 0.54 mmol·L^{-1} DBT and different glycerol supplementation (0, 0.05, 0.5, 5, 50, 200, and 500 mmol·L^{-1}).

in the four treatments (Fig. 2, Table 2). RmlD catalyzes the final step from dTDP-4-keto-6-deoxy-*L*-mannose to dTDP-rhamnose. The changes in the relative protein abundance of RmlD in the different treatments were significant ($p < 0.05$), and the log FC was upregulated. The log FC represents the effect of the glycerol × DBT interaction term. Its upregulation indicates that this interaction had a positive effect on the treatments containing this term. The enzyme RmlC that catalyzes the previous step in the pathway was also upregulated. The relative abundance of both RmlD and RmlC suggests that the synthesis of RL sugar precursors is not inhibited by the RL biosynthesis inhibitor OC.

Enzymes from the FAS II and/or β-oxidation pathways were detected in the four treatments (Fig. 2, Table 2). FabG is the enzyme catalyzing the final step in *R*-3-hydroxydecanoyl-ACP synthesis via the FAS II pathway [46]. The relative abundance of FabG was > 1 in all treatments, indicating that this protein was detected. However, the *p*-value was above 0.05, meaning that their relative abundances did not show significant differences (Table 2). The preceding step catalyzed by FabF was upregulated in treatment (C). The β-oxidation enzymes FadB and FadE were abundant in treatment (C) (Table 2). The results indicate that the later stages in the FAS II and β-oxidation pathways are active in C3 at day 2 of cultivation.

RhlA produces 3-hydroxy alkanoic acid (HAA), which is then utilized by RhlB for mono-rhamnolipid biosynthesis [47]. RhlA was identified and the log FC showed upregulation. Rhamnosyltransferases RhlB and RhlC were also identified (Table 2). RhlB and RhlC are involved in the direct formation of mono-rhamnolipids [48,49] and di-RLs [50], respectively. The proteins identified in Table 2 suggest that glycerol induces lipid precursors for the biosynthesis of RL biosurfactants in C3 cells. The data suggest the involvement of both the FAS II and β-oxidation pathways in the synthesis of the lipid precursor. However, it is uncertain which pathway dominates, as these pathways have additional roles in the cells, such as cell proliferation.

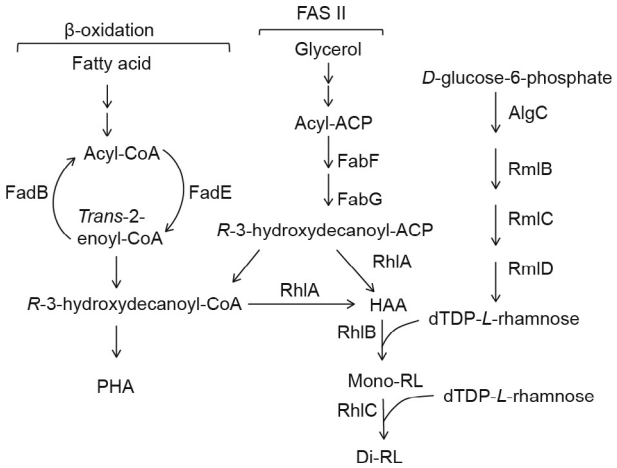

Fig. 2. Identification of proteins involved on RL biosynthesis in *Burkholderia* sp. C3. Bolded proteins showed upregulation in the glycerol×DBT interaction term (log FC). FadB: enoyl-CoA hydratase/3-hydroxyacyl-CoA dehydrogenase; FadE: acyl-CoA dehydrogenase; FabF: β-oxoacyl-ACP synthase 2; ACP: acyl carrier protein; FabG: 3-oxoacyl-ACP-reductase; RhlA: HAA synthase; HAA: 3-hydroxy alkanoic acid; RhlB: rhamnosyltransferase 1; RhlC: rhamnosyltransferase 2; AlgC: phosphoglucomutase/phosphomannomutase; RmlB: dTDP-glucose 4,6-dehydratase; RmlC: dTDP-4-dehydrorhamnose-3,5-epimerase; RmlD: dTDP-4-dehydrorhamnose reductase.

3.3. Enhanced DBT biodegradation in Burkholderia sp. C3 is affected by RL biosynthesis and its inhibition

DBT is hydrophobic [6] and its bioavailability is the first requirement for biodegradation [15]. DBT solubilization and foam formation were observed in the cultures when glycerol was supplemented. Such observations suggest the secretion of a surfactant agent. Our proteomics results indicate that the RL biosurfactant biosynthesis pathway is active in C3. Thus, the relevance of RLs to the enhanced DBT biodegradation induced by glycerol was investigated with an orcinol assay [51].

Gutierrez et al. [25] showed that inhibition of RhlA by bromoalkanoic acids suppresses the production of RLs and PHA in *Pseudomonas* species, and that this inhibition is dependent on the

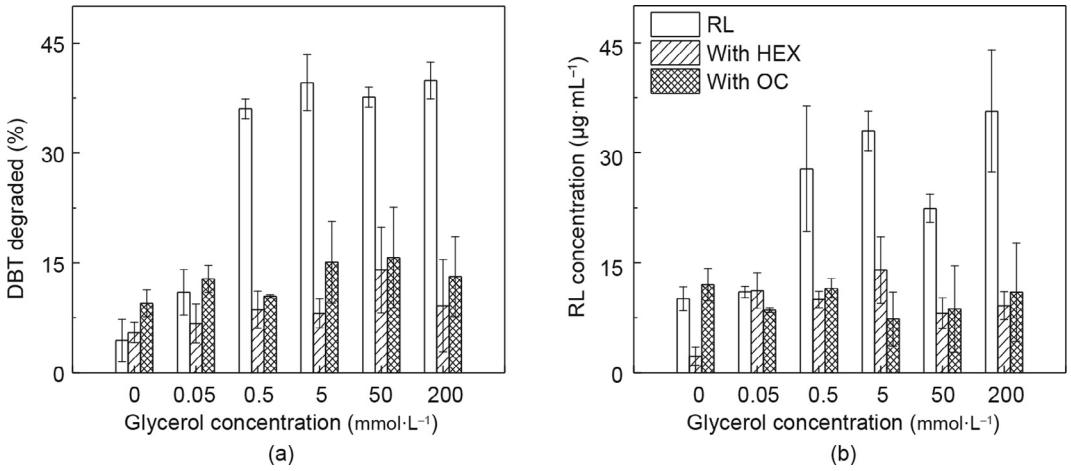

Fig. 3. Association between (a) the amount of RL secreted at day 2 and (b) the amount of DBT degraded at day 1 by *Burkholderia* sp. C3 cultivated without inhibitor, with 2 mmol·L^{-1} of HEX or 2 mmol·L^{-1} of OC and different glycerol concentrations (0, 0.05, 0.5, 5, 50, and 200 mmol·L^{-1}).

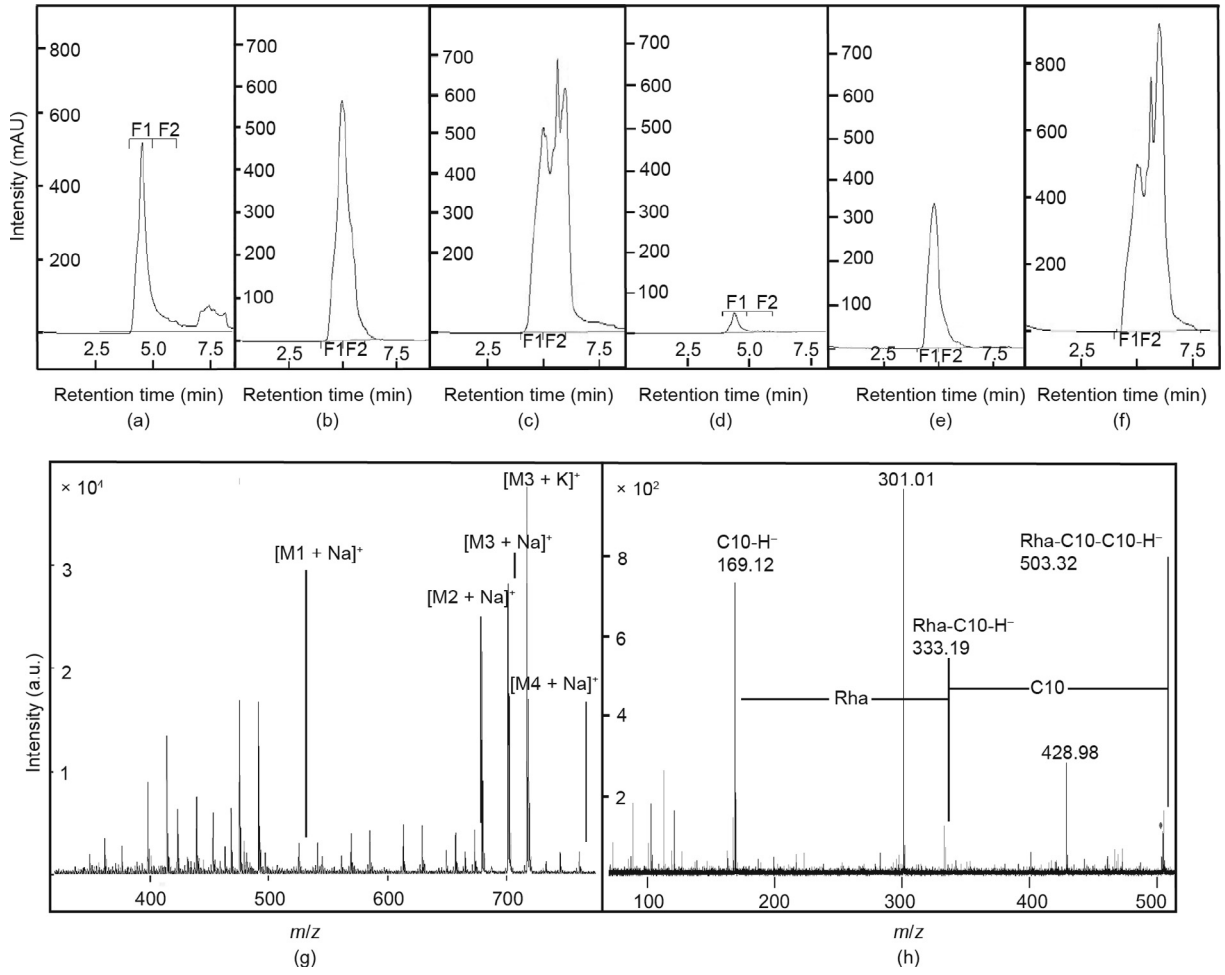

Fig. 4. HPLC chromatograms of RLs secreted by *Burkholderia* sp. C3 cultivated with (a) 0.54 mmol·L^{-1} DBT and 50 mmol·L^{-1} glycerol, with (b) 2 mmol·L^{-1} of HEX, or (c) 2 mmol·L^{-1} of OC, and cultivated with (d) 0.54 mmol·L^{-1} DBT, with (e) 2 mmol·L^{-1} of HEX, or (f) 2 mmol·L^{-1} of OC. (g) MALDI-TOF-MS of 4 RL congeners (M1, M2, M3, and M4) identified from HPLC chromatogram a, fraction 2 (F2), and (h) LC-Q-TOF-MS2 of Rha-C10-C10 (M1).

bromoalkanoic acid used. Inhibition of RLs and PHA has also been described in the literature [24]. 2-Bromoalkanoic acids (HEX or OC) were therefore used to probe the roles of RLs in DBT biodegradation by the strain C3. If RLs play a role in DBT biodegradation, HEX and OC should decrease DBT biodegradation via RL biosynthesis inhibition. An increase in RL secretion was quantified when the strain C3 was cultivated in the glycerol/DBT mixture relative to cultivation in DBT alone. RL biosynthesis and secretion, induced by varying concentrations of glycerol (Fig. 3(a)), were strongly associated with the amount of DBT degraded (Fig. 3(b)), as was RL biosynthesis inhibition by HEX and OC. The results agreed with the proteomics findings; RL biosynthesis occurs in C3 and is strongly associated with its biodegradation ability.

3.4. RL congeners are secreted by Burkholderia sp. C3

An RL standard containing a mixture of Rha-Rha-C10-C10 and Rha-C10-C10 congeners was used to identify RLs in experimental samples. RL congeners were eluted between 4 and 6 min (Fig. 4). The HPLC chromatograms of the experimental samples matched well with those of the RL standards (data not shown). Two fractions named F1 and F2 were collected from the experimental samples with 0.5 $mmol \cdot L^{-1}$ DBT and either 50 or 0 $mmol \cdot L^{-1}$ glycerol. Fractions from the cultures treated with 2 $mmol \cdot L^{-1}$ of HEX or OC inhibitors were also collected. The peak intensity on the HPLC chromatogram of the extract from the 50 $mmol \cdot L^{-1}$ glycerol-supplemented culture was approximately 10-fold higher than that on the 0 $mmol \cdot L^{-1}$ glycerol HPLC chromatogram. Glycerol induced an increase in RL production. It is noteworthy that multiple peaks occurred at the OC chromatograms (Figs. 4(c) and (f)).

The most intense peaks were assigned to RL congeners. In the 50 $mmol \cdot L^{-1}$ glycerol samples, C3 secreted the congeners Rha-C10-C10 ($M1 + Na^+$), Rha-Rha-C10-C10 ($M2 + Na^+$), Rha-Rha-C10-C12—which were identified in sodium ($M3 + Na^+$) or potassium ($M3 + K^+$) adduct ion forms—and Rha-Rha-C12-C12 ($M4 + Na^+$). The mono-rhamnolipid congener Rha-C12-C12 was identified in the 0 $mmol \cdot L^{-1}$ glycerol samples and in the samples with HEX or OC inhibitors (either in 50 or 0 $mmol \cdot L^{-1}$ glycerol) (data not shown). The peaks M1 and M2 were confirmed with MS/MS. The mass spectrum of Rha-C10-C10 is shown in Fig. 4(h). Loss of C10 acyl chain and rhamnose sugar fragments (Rha) were observed. It is concluded that glycerol supports C3 cell growth and enhances the biodegradation of DBT via an RL-mediated mechanism.

Our findings suggest that the utilization of glycerol could lead to the effective biodegradation of persistent organic pollutants—including organochlorine pesticides and PAHs—in contaminated soil and could thus be used in the restoration of land functionality, making it available for agricultural purposes. This biostimulation strategy could be applied in combination with the bioaugmentation of a suitable microbial consortium. Our findings suggest that glycerol may trigger a superior response in a bacterial population with a mixture of PAH degraders and RL producers. An initial analysis of the bacterial population and cellular respiration, along with PAH biodegradation monitoring over time, would be required for a proper assessment of the bioremediation site.

4. Conclusions

The amphipathic properties of RLs suggest multiple functions for RL producers and PAH degraders. Some of the functions are related to hydrophobic chemical solubilization, chemical uptake, and biological assimilation. Our studies indicated a 30% increase in DBT biodegradation with glycerol biostimulation after one day of incubation. This enhancement was associated with increased di-RL biosynthesis by *Burkholderia* sp. C3 and bacterial growth. In addition, we report the use of 2-bromoalkanoic acid for RL biosynthesis inhibition in a *Burkholderia* species. To our knowledge, this is the first report correlating glycerol supplementation to DBT biodegradation and RL biosynthesis. The results suggest a potential practicality of the biostimulation strategy described here to improve bioremediation efficiencies and facilitate such processes.

Acknowledgements

This work was supported in part by Grant N00014-12-1-0496 from the Office of Naval Research and a subcontract with the Western Center for Agricultural Health and Safety (NIOSH grant 2U54OH007550). The authors thank Dr. Margaret R. Baker for her assistance with MALDI/TOF.

Compliance with ethics guidelines

Camila A. Ortega Ramirez, Abraham Kwan, and Qing X. Li declare that they have no conflict of interest or financial conflicts to disclose.

Nomenclature

ACN	acetonitrile
CoA	coenzyme A
FabZ	3-hydroxy-ACP-dehydratase
FDR	false discovery rate
HEX	2-bromohexanoic acid
HPLC	high-performance liquid chromatograph
HSD	honestly significant difference
LSD	least significant difference
DHB	dihydroxybenzoic acid
DP	degree of polymerization
OC	2-bromooctanoic acid
DBT	dibenzothiophene
FAS II	*de novo* fatty acid synthesis
FadB	enoyl-CoA hydratase/3-hydroxyacyl-CoA dehydrogenase
FadE	acyl-CoA dehydrogenase
FabF	β-oxoacyl-ACP synthase 2
ACP	acyl carrier protein
FabG	3-oxoacyl-ACP-reductase
RhlA	HAA synthase
HAA	3-hydroxy alkanoic acid
RhlB	rhamnosyltransferase 1
RhlC	rhamnosyltransferase 2
AlgC	phosphoglucomutase/phosphomannomutase
RmlB	dTDP-glucose 4,6-dehydratase
RmlC	dTDP-4-dehydrorhamnose-3,5-epimerase
RmlD	dTDP-4-dehydrorhamnose reductase
MALDI/TOF	matrix-assisted laser desorption ionization time-of-flight
LC-Q-TOF-MS	liquid chromatograph-quadrupole time-of-flight mass spectrometer
MM	minimal medium
MS	mass spectrometry
PAH	polycyclic aromatic hydrocarbon
PHA	polyhydroxyalkanoic acid
RL	rhamnolipid

References

[1] Kampman B, Brouwer F, Schepersa B. Agricultural land availability and demand in 2020: a global analysis of drivers and demand for feedstock, and agricultural land availability. Delft: CE Delft; 2008.
[2] Gereslassie T, Workineh A, Liu X, Yan X, Wang J. Occurrence and ecological and human health risk assessment of polycyclic aromatic hydrocarbons in soils

from Wuhan, central China. Int J Environ Res Public Health 2018;15(12):E2751.
[3] Lim MW, Lau EV, Poh PE. A comprehensive guide of remediation technologies for oil contaminated soil—present works and future directions. Mar Pollut Bull 2016;109(1):14–45.
[4] Andreolli M, Lampis S, Poli M, Gullner G, Biró B, Vallini G. Endophytic *Burkholderia fungorum* DBT1 can improve phytoremediation efficiency of polycyclic aromatic hydrocarbons. Chemosphere 2013;92(6):688–94.
[5] Li M, Wang TG, Simoneit BR, Shi S, Zhang L, Yang F. Qualitative and quantitative analysis of dibenzothiophene, its methylated homologues, and benzonaphthothiophenes in crude oils, coal, and sediment extracts. J Chromatogr A 2012;1233:126–36.
[6] Incardona JP, Collier TK, Scholz NL. Defects in cardiac function precede morphological abnormalities in fish embryos exposed to polycyclic aromatic hydrocarbons. Toxicol Appl Pharmacol 2004;196(2):191–205.
[7] Seo JS, Keum YS, Li QX. Bacterial degradation of aromatic compounds. Int J Environ Res Public Health 2009;6(1):278–309.
[8] Brinkmann M, Maletz S, Krauss M, Bluhm K, Schiwy S, Kuckelkorn J, et al. Heterocyclic aromatic hydrocarbons show estrogenic activity upon metabolization in a recombinant transactivation assay. Environ Sci Technol 2014;48(10):5892–901.
[9] Li F, Zhu L, Wang L, Zhan Y. Gene expression of an arthrobacter in surfactant-enhanced biodegradation of a hydrophobic organic compound. Environ Sci Technol 2015;49(6):3698–704.
[10] Demanèche S, Meyer C, Micoud J, Louwagie M, Willison JC, Jouanneau Y. Identification and functional analysis of two aromatic-ring-hydroxylating dioxygenases from a *Sphingomonas* strain that degrades various polycyclic aromatic hydrocarbons. Appl Environ Microbiol 2004;70(11):6714–25.
[11] Singleton DR, Hu J, Aitken MD. Heterologous expression of polycyclic aromatic hydrocarbon ring-hydroxylating dioxygenase genes from a novel pyrene-degrading betaproteobacterium. Appl Environ Microbiol 2012;78(10):3552–9.
[12] Eibes G, Cajthaml T, Moreira MT, Feijoo G, Lema JM. Enzymatic degradation of anthracene, dibenzothiophene and pyrene by manganese peroxidase in media containing acetone. Chemosphere 2006;64(3):408–14.
[13] Szulc A, Ambrożewicz D, Sydow M, Ławniczak Ł, Piotrowska-Cyplik A, Marecik R, et al. The influence of bioaugmentation and biosurfactant addition on bioremediation efficiency of diesel-oil contaminated soil: feasibility during field studies. J Environ Manage 2014;132:121–8.
[14] Noordman WH, Janssen DB. Rhamnolipid stimulates uptake of hydrophobic compounds by *Pseudomonas aeruginosa*. Appl Environ Microbiol 2002;68(9):4502–8.
[15] Makkar RS, Rockne KJ. Comparison of synthetic surfactants and biosurfactants in enhancing biodegradation of polycyclic aromatic hydrocarbons. Environ Toxicol Chem 2003;22(10):2280–92.
[16] Elliot R, Singhal N, Swift S. Surfactants and bacterial bioremediation of polycyclic aromatic hydrocarbon contaminated soil—unlocking the targets. Crit Rev Environ Sci Technol 2010;41(1):78–124.
[17] Perfumo A, Banat IM, Canganella F, Marchant R. Rhamnolipid production by a novel thermophilic hydrocarbon-degrading *Pseudomonas aeruginosa* AP02-1. Appl Microbiol Biotechnol 2006;72(1):132.
[18] Peng F, Liu Z, Wang L, Shao Z. An oil-degrading bacterium: *Rhodococcus erythropolis* strain 3C-9 and its biosurfactants. J Appl Microbiol 2007;102(6):1603–11.
[19] Xia W, Du Z, Cui Q, Dong H, Wang F, He P, et al. Biosurfactant produced by novel *Pseudomonas* sp. WJ6 with biodegradation of *n*-alkanes and polycyclic aromatic hydrocarbons. J Hazard Mater 2014;276:489–98.
[20] Bodour AA, Drees KP, Maier RM. Distribution of biosurfactant-producing bacteria in undisturbed and contaminated arid southwestern soils. Appl Environ Microbiol 2003;69(6):3280–7.
[21] Seo JS, Keum YS, Harada RM, Li QX. Isolation and characterization of bacteria capable of degrading polycyclic aromatic hydrocarbons (PAHs) and organophosphorus pesticides from PAH-contaminated soil in Hilo, Hawaii. J Agric Food Chem 2007;55(14):5383–9.
[22] Tittabutr P, Cho IK, Li QX. Phn and Nag-like dioxygenases metabolize polycyclic aromatic hydrocarbons in *Burkholderia* sp. C3. Biodegradation 2011;22(6):1119–33.
[23] Seo JS, Keum YS, Hu Y, Lee SE, Li QX. Degradation of phenanthrene by *Burkholderia* sp. C3: initial 1,2- and 3,4-dioxygenation and meta- and ortho-cleavage of naphthalene-1,2-diol. Biodegradation 2007;18(1):123–31.
[24] Abdel-Mawgoud AM, Lépine F, Déziel E. A stereospecific pathway diverts ß-oxidation intermediates to the biosynthesis of rhamnolipid biosurfactants. Chem Biol 2014;21(1):156–64.
[25] Gutierrez M, Choi MH, Tian B, Xu J, Rho JK, Kim MO, et al. Simultaneous inhibition of rhamnolipid and polyhydroxyalkanoic acid synthesis and biofilm formation in *Pseudomonas aeruginosa* by 2-bromoalkanoic acids: effect of inhibitor alkyl-chain-length. PLoS ONE 2013;8(9):e73986.
[26] Bastiaens L, Springael D, Wattiau P, Harms H, deWachter R, Verachtert H, et al. Isolation of adherent polycyclic aromatic hydrocarbon (PAH)-degrading bacteria using PAH-sorbing carriers. Appl Environ Microbiol 2000;66(5):1834–43.
[27] Akhtar N, Ghauri MA, Anwar MA, Akhtar K. Analysis of the dibenzothiophene metabolic pathway in a newly isolated *Rhodococcus* spp. FEMS Microbiol Lett 2009;301(1):95–102.
[28] Dephoure N, Gygi SP. A solid phase extraction-based platform for rapid phosphoproteomic analysis. Methods 2011;54(4):379–86.
[29] Tabb DL, Fernando CG, Chambers MC. MyriMatch: highly accurate tandem mass spectral peptide identification by multivariate hypergeometric analysis. J Proteome Res 2007;6(2):654–61.
[30] Ma ZQ, Dasari S, Chambers MC, Litton MD, Sobecki SM, Zimmerman LJ, et al. IDPicker 2.0: improved protein assembly with high discrimination peptide identification filtering. J Proteome Res 2009;8(8):3872–81.
[31] Holman JD, Ma ZQ, Tabb DL. Identifying proteomic LC-MS/MS data sets with bumbershoot and IDPicker. Curr Protoc Bioinf 2012;37(1):13–7.
[32] Griffin NM, Yu J, Long F, Oh P, Shore S, Li Y, et al. Label-free, normalized quantification of complex mass spectrometry data for proteomic analysis. Nat Biotechnol 2010;28(1):83–9.
[33] Love MI, Huber W, Anders S. Moderated estimation of fold change and dispersion for RNA-seq data with DESeq2. Genome Biol 2014;15(12):550.
[34] Irie Y, Parsek MR. LC/MS/MS-based quantitative assay for the secondary messenger molecule, c-di-GMP. Pseudomonas Methods Protoc 2014;1149:271–9.
[35] Laabei M, Jamieson WD, Lewis SE, Diggle SP, Jenkins AT. A new assay for rhamnolipid detection-important virulence factors of *Pseudomonas aeruginosa*. Appl Microbiol Biotechnol 2014;98(16):7199–209.
[36] Price NP, Ray KJ, Vermillion K, Kuo TM. MALDI-TOF mass spectrometry of naturally occurring mixtures of monorhamnolipids and dirhamnolipids. Carbohydr Res 2009;344(2):204–9.
[37] Price NP. Oligosaccharide structures studied by hydrogen-deuterium exchange and MALDI-TOF mass spectrometry. Anal Chem 2006;78(15):5302–8.
[38] Abdel-Mawgoud AM, Lépine F, Déziel E. Rhamnolipids: diversity of structures, microbial origins and roles. Appl Microbiol Biotechnol 2010;86(5):1323–36.
[39] Hennessee CT, Li QX. Effects of polycyclic aromatic hydrocarbon mixtures on degradation, gene expression, and metabolite production in four *Mycobacterium* species. Appl Environ Microbiol 2016;82(11):3357–69.
[40] Deutscher J. The mechanisms of carbon catabolite repression in bacteria. Curr Opin Microbiol 2008;11(2):87–93.
[41] Wolfe A, Shimer GH Jr, Meehan T. Polycyclic aromatic hydrocarbons physically intercalate into duplex regions of denatured DNA. Biochemistry 1987;26(20):6392–6.
[42] Dabestani R, Ivanov IN. A compilation of physical, spectroscopic and photophysical properties of polycyclic aromatic hydrocarbons. Photochem Photobiol 1999;70(1):10–34.
[43] Dobler L, Vilela LF, Almeida RV, Neves BC. Rhamnolipids in perspective: gene regulatory pathways, metabolic engineering, production and technological forecasting. N Biotechnol 2016;33(1):123–35.
[44] Costa SG, Déziel E, Lépine F. Characterization of rhamnolipid production by *Burkholderia glumae*. Lett Appl Microbiol 2011;53(6):620–7.
[45] Choi MH, Xu J, Gutierrez M, Yoo T, Cho YH, Yoon SC. Metabolic relationship between polyhydroxyalkanoic acid and rhamnolipid synthesis in *Pseudomonas aeruginosa*: comparative ^{13}C NMR analysis of the products in wild-type and mutants. J Biotechnol 2011;151(1):30–42.
[46] Rehm BH, Mitsky TA, Steinbüchel A. Role of fatty acid *de novo* biosynthesis in polyhydroxyalkanoic acid (PHA) and rhamnolipid synthesis by pseudomonads: establishment of the transacylase (PhaG)-mediated pathway for PHA biosynthesis in *Escherichia coli*. Appl Environ Microbiol 2001;67(7):3102–9.
[47] Zhu K, Rock CO. RhlA converts ß-hydroxyacyl-acyl carrier protein intermediates in fatty acid synthesis to the ß-hydroxydecanoyl-ß-hydroxydecanoate component of rhamnolipids in *Pseudomonas aeruginosa*. J Bacteriol 2008;190(9):3147–54.
[48] Tavares LF, Silva PM, Junqueira M, Mariano DC, Nogueira FC, Domont GB, et al. Characterization of rhamnolipids produced by wild-type and engineered *Burkholderia kururiensis*. Appl Microbiol Biotechnol 2013;97(5):1909–21.
[49] Ochsner UA, Reiser J, Fiechter A, Witholt B. Production of *Pseudomonas aeruginosa* rhamnolipid biosurfactants in heterologous hosts. Appl Environ Microbiol 1995;61(9):3503–6.
[50] Rahim R, Ochsner UA, Olvera C, Graninger M, Messner P, Lam JS, et al. Cloning and functional characterization of the *Pseudomonas aeruginosa rhlC* gene that encodes rhamnosyltransferase 2, an enzyme responsible for di-rhamnolipid biosynthesis. Mol Microbiol 2001;40(3):708–18.
[51] Déziel E, Lépine F, Milot S, Villemur R. Mass spectrometry monitoring of rhamnolipids from a growing culture of *Pseudomonas aeruginosa* strain 57RP. Biochim Biophys Acta Mol Cell Biol Lipids 2000;1485(2–3):145–52.